The Astrophysical Journal, 677:127–136, 2008 April 10

THE HOST GALAXIES AND BLACK HOLES OF TYPICAL $z \sim 0.5$–1.4 AGNs

Almudena Alonso-Herrero,[1,2] Pablo G. Pérez-González,[2,3] George H. Rieke,[2] David M. Alexander,[4] Jane R. Rigby,[5] Casey Papovich,[2] Jennifer L. Donley,[2] and Dimitra Rigopoulou[6]

Received 2007 August 27; accepted 2007 December 17

ABSTRACT

We study the stellar and star formation properties of the host galaxies of 58 X-ray–selected AGNs in the GOODS portion of the *Chandra* Deep Field South (CDF-S) region at $z \sim 0.5$–1.4. The AGNs are selected such that their rest-frame UV to near-infrared spectral energy distributions (SEDs) are dominated by stellar emission; i.e., they show a prominent 1.6 μm bump, thus minimizing the AGN emission "contamination." This AGN population comprises approximately 50% of the X-ray–selected AGNs at these redshifts. We find that AGNs reside in the most massive galaxies at the redshifts probed here. Their characteristic stellar masses ($M_* \sim 7.8 \times 10^{10}$ and $M_* \sim 1.2 \times 10^{11}\ M_\odot$ at median redshifts of 0.67 and 1.07, respectively) appear to be representative of the X-ray–selected AGN population at these redshifts and are intermediate between those of local type 2 AGNs and high-redshift ($z \sim 2$) AGNs. The inferred black hole masses ($M_{\rm BH} \sim 2 \times 10^8\ M_\odot$) of typical AGNs are similar to those of optically identified quasars at similar redshifts. Since the AGNs in our sample are much less luminous ($L_{2-10\,\rm keV} < 10^{44}$ erg s^{-1}) than quasars, typical AGNs have low Eddington ratios ($\eta \sim 0.01$–0.001). This suggests that, at least at intermediate redshifts, the cosmic AGN "downsizing" is due to both a decrease in the characteristic stellar mass of typical host galaxies and less efficient accretion. Finally, there is no strong evidence in AGN host galaxies for either highly suppressed star formation (expected if AGNs played a role in quenching star formation) or elevated star formation when compared to mass-selected (i.e., IRAC-selected) galaxies of similar stellar masses and redshifts.

Subject headings: galaxies: active — galaxies: evolution — galaxies: high-redshift — galaxies: stellar content — infrared: galaxies

Online material: color figures

1. INTRODUCTION

One of the challenges faced by galaxy formation models is to explain the population of today's red massive quiescent elliptical galaxies. In the current hierarchical galaxy formation paradigm, massive galaxies are formed via mergers of less massive galaxies, which in turn fuel intense star formation and feed massive black holes. One of the main difficulties is to find mechanisms to stop the processes of intense star formation and to allow galaxies to migrate from the so-called blue cloud, or late-type star-forming galaxies, to the so-called red sequence, or early-type quiescent galaxies (see, e.g., Bell et al. 2004, 2007). Feedback from active galactic nuclei (AGNs) has been proposed as an efficient process for suppressing any further star formation during the late stages of galaxy evolution, while still allowing black holes to continue to grow (see, e.g., Springel et al. 2005; Croton et al. 2006). See Hopkins et al. (2007 and references therein) for a detailed discussion of this and other related issues.

Some tantalizing evidence of the possible role of AGNs in galaxy evolution is the location of local optically selected AGNs (e.g., Salim et al. 2007; Martin et al. 2007) and moderate-z X-ray–selected AGNs (Sánchez et al. 2004; Nandra et al. 2007) in the transition between the red sequence and the top of the blue cloud, which is the region also known as the "green valley." These intermediate colors may indicate that AGNs play a role in causing or maintaining the quenching of star formation. However, in the local universe, AGNs with strongly accreting black holes tend to be hosted in massive galaxies with blue (i.e., star-forming) disks and young bulges (Kauffmann et al. 2003b, 2007), which implies a close link between the growth of black holes and bulges. Clearly, the relationship between AGNs and star formation is a matter of strong debate.

About half of the sources with X-ray luminosities of $\gtrsim 10^{41}$ erg s^{-1} (i.e., that are suggestive of the presence of a moderately luminous AGN) that have been detected in deep ($\geq$1 Ms) X-ray surveys do not show broad lines or high-excitation lines characteristic of AGNs in their optical spectra (see, e.g., Barger et al. 2003; Cohen 2003; Szokoly et al. 2004; review by Brandt & Hasinger 2005). Since the AGN emission of these optically dull AGNs does not dominate their rest-frame UV to near-infrared (NIR) emission (Rigby et al. 2006), they are the ideal targets with which to study their host galaxies and investigate the role of AGNs in galaxy evolution.

In this paper we study the host galaxies of X-ray–selected AGNs with stellar-dominated spectral energy distributions (SEDs) at intermediate redshifts ($0.5 < z < 1.4$) in the *Chandra* Deep Field South (CDF-S), using UV, optical, NIR, and *Spitzer* data. The AGN host galaxy properties are then compared with those of IRAC-selected (i.e., stellar mass–selected) galaxies at similar distances that were studied by Pérez-González et al. (2008). Throughout this work, we assumed the following cosmology: $H_0 = 70$ km s^{-1} Mpc^{-1}, $\Omega_M = 0.3$, and $\Omega_\Lambda = 0.7$.

2. SAMPLE SELECTION AND DATA

We first started with all the CDF-S X-ray sources (Giacconi et al. 2002; Alexander et al. 2003) with spectroscopic and photometric redshifts in the range $0.5 < z < 1.4$ (Zheng et al. 2004). Then we

[1] Departamento de Astrofísica Molecular e Infrarroja, Instituto de Estructura de la Materia, CSIC, E-28006 Madrid, Spain; aalonso@damir.iem.csic.es.
[2] Steward Observatory, University of Arizona, Tucson, AZ 85721.
[3] Departamento de Astrofísica y Ciencias de la Atmósfera, Universidad Complutense de Madrid, E-28040 Madrid, Spain.
[4] Department of Physics, University of Durham, Durham, DH1 3LE, UK.
[5] Observatories of the Carnegie Institution of Washington, Pasadena, CA 91101.
[6] Department of Astrophysics, Keble Road, Oxford OX1 3RH, UK.

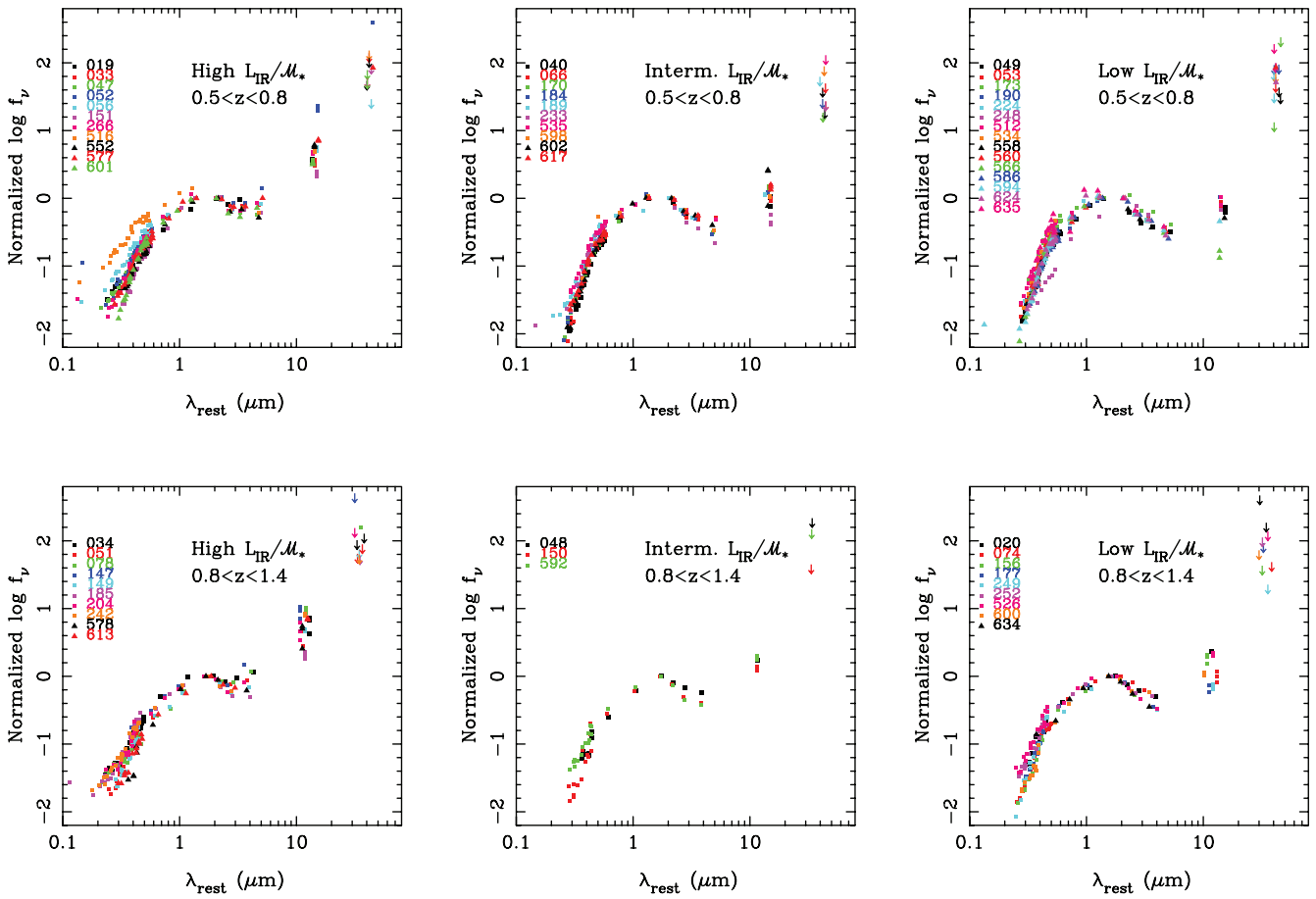

FIG. 1.— *Top*: Rest-frame SEDs, normalized at ~1–2 μm, of CDF-S AGNs at $0.5 < z < 0.8$, whose integrated UV through NIR SEDs are dominated by stellar emission. The numbers given next to the symbols in the upper left corners of the plots are the Giacconi et al. (2002) IDs. From left to right, galaxies are plotted for decreasing IR luminosity–to–stellar mass ratios relative to the mass dependence found for IRAC-selected galaxies (see more details in § 5.2). These ratios are a measure of the specific SFR if the IR luminosity is not dominated by AGN emission. *Bottom*: Same as above, but for AGNs at $0.8 < z < 1.4$.

restricted our sample to those X-ray sources in the Great Observatories Origins Deep Survey (GOODS) portion of the CDF-S region that has the deepest *Spitzer* IRAC (Fazio et al. 2004) and MIPS (Rieke et al. 2004) observations (see Pérez-González et al. 2008). We cross-correlated the positions of the X-ray sources with the IRAC-selected (for simultaneous detections at 3.6 and 4.5 μm) galaxies of Pérez-González et al. (2008), using a separation of $\leq 1.5''$. The 75% completeness limits for the CDF-S field in this sample are 1.6 and 1.4 μJy at 3.5 and 4.5 μm, respectively.

We also used the CDF-S photometric catalogs of Pérez-González et al. (2008) to construct the SEDs of the X-ray sources. These catalogs include data from the two other IRAC bands, as well as UV, optical, NIR, and *Spitzer* MIPS 24 μm data (see Pérez-González et al. [2005, 2008] for a complete description of the data set and source matching). The MIPS 24 μm catalog is 75% complete down to 80 μJy. Finally, we cross-correlated the X-ray sources with the *Spitzer* MIPS 70 μm catalog for the CDF-S (Papovich et al. 2007), which is 50% complete for sources with flux densities down to $f_\nu(70\ \mu\text{m}) \sim 3.9$ mJy.

Out of the 112 X-ray sources with IRAC detections in the field described above, we selected for this study AGNs with stellar-dominated UV through NIR SEDs, and in particular those with a strong 1.6 μm bump. Our selection thus excluded X-ray sources with AGN-dominated SEDs, such as IR power-law galaxies (Alonso-Herrero et al. 2006; Donley et al. 2007), IRAC color-color–selected AGNs (Lacy et al. 2004; Stern et al. 2005), and galaxies without a prominent 1.6 μm bump (e.g., Daddi et al. 2007). We also removed from our sample X-ray sources with nearby companions of similar brightness that could contaminate the observed mid-IR (MIR) SEDs, particularly the IRAC bands. The final sample contains 58 AGNs.

Most (52 out of 58) of the AGNs in our sample have spectroscopic redshifts and type classifications (Szokoly et al. 2004; Vanzella et al. 2006). The majority (46 out of 52) are classified as optically dull; that is, AGNs that do not show any evidence for accretion from their optical spectra. These include AGNs classified as low-excitation and absorption-line AGNs (see Szokoly et al. 2004). The remaining six AGNs with spectroscopic information show high-excitation lines or broad lines (Szokoly et al. 2004) and will be referred to as optically active AGNs. For the six AGNs in our sample that do not have spectroscopic information, we estimated photometric redshifts (see § 3).

The rest-frame SEDs of the 58 AGNs are shown in Figure 1 for two different redshift bins: $0.5 < z < 0.8$ and $0.8 < z < 1.4$, which correspond to approximately similar ranges of cosmic times for the assumed cosmology.

The selected AGNs have rest-frame absorption-corrected hard (2–10 keV) X-ray luminosities that are above 10^{41} erg s^{-1} (from Tozzi et al. 2006). Figure 2 compares the X-ray column densities with the absorption-corrected hard X-ray luminosities (from Tozzi et al. 2006) for all the X-ray sources (*circles*) detected by IRAC in the GOODS field. We marked the AGNs with stellar-dominated SEDs that were selected for this study with filled circles.

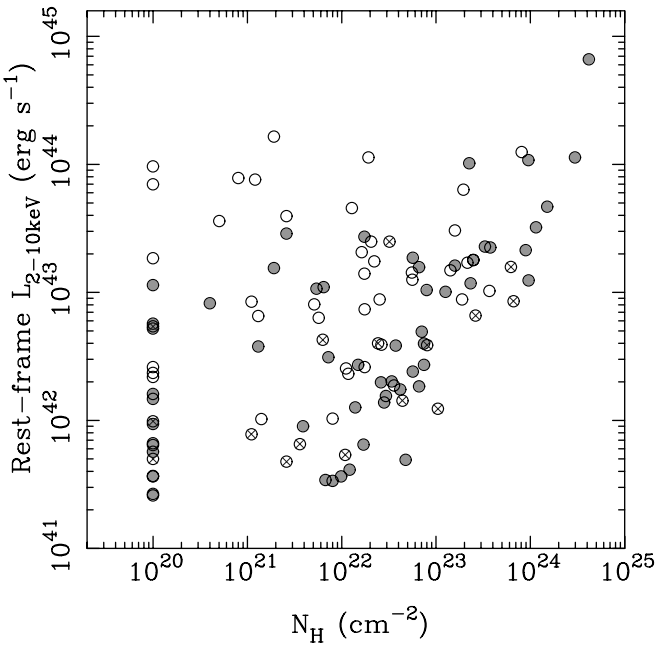

FIG. 2.— X-ray column density vs. rest-frame absorption-corrected hard X-ray luminosity (both from Tozzi et al. 2006) for the X-ray–selected AGNs (*circles*) in GOODS that were detected by *Spitzer* at $0.5 < z < 1.4$. Our sample of AGNs with stellar-dominated SEDs are shown as filled circles. We also mark with crosses the optically dull AGNs with nearby companions that were not included in the present analysis. When the X-ray column densities were estimated by Tozzi et al. (2006) to be zero, we plot them at 10^{20} cm^{-2}. [*See the electronic edition of the Journal for a color version of this figure*.]

Figure 2 clearly shows that a large fraction of AGNs with hard X-ray luminosities below $\sim 10^{43}$ erg s^{-1} have SEDs that are dominated by stellar emission (see also Donley et al. 2007). At higher hard X-ray luminosities, only those AGNs with large X-ray column densities have stellar SEDs (see also Polletta et al. 2006, 2007). At low absorptions ($N_H < 10^{22}$ cm^{-2}), the AGN emission becomes more apparent in the integrated SEDs, but there are some X-ray sources that have both low values of N_H and stellar-dominated SEDs. These sources will be studied in more detail in § 4.1.

The X-ray properties of our sample of AGNs (Fig. 2) are consistent with recent findings on the nature of optically dull AGNs. Rigby et al. (2006) estimated that in $\sim$50% of all optically dull AGNs, the AGN emission lines could be diluted by the stellar emission from the host galaxy (see also Moran et al. 2002), whereas in the rest, extinction from the host galaxy may be responsible for hiding the AGN optical lines. The latter conclusion was based on a comparison of the inclination angle distributions of the host galaxies of optically dull and optically active AGNs. Recently, Caccianiga et al. (2007) proposed that the most likely explanation for optical dullness at low X-ray luminosities is dilution by a massive host galaxy, while at high X-ray luminosities the dullness is due to absorption.

3. MODELING OF THE STELLAR EMISSION AT $\lambda_{rest} < 4$ μm

This section describes briefly (see Pérez-González et al. 2008 for a full description) the procedure for modeling the SEDs at wavelengths of $\lambda_{rest} < 4$ μm. This modeling is general to the IRAC-selected sample of Pérez-González et al. (2008) from which we extracted the stellar masses (this section) and the star formation rates (§ 4.2) for our sample of AGNs. The method involves a two-step process in which the galaxies with spectroscopic redshifts are fitted first and are then used as templates to fit the SEDs (and photometric redshifts) of those galaxies without spectroscopic redshifts.

For galaxies with spectroscopic redshifts, the stellar emission is generated with the PEGASE code (Fioc & Rocca-Volmerange 1997), under the assumption of a Salpeter initial mass function (IMF; Salpeter 1955) between 0.1 and 100 $M_\odot$. We assumed that the stellar emission of the galaxies can be described with one or two stellar populations. In the case of the model with one stellar population, the star formation rate (SFR) is modeled with a declining exponential [$\mathrm{SFR}(t) \propto \exp^{-t/\tau}$]. The four free parameters to be fitted are the extinction (using the Calzetti et al. 2000 law), the metallicity, the timescale of the exponential law (τ), and the age (t) of the stellar population. In the case with two stellar populations, the old stellar population is described as for the model with one stellar population (four free parameters), and the young stellar population is assumed to have been formed in an instantaneous burst, with three free parameters: extinction, metallicity, and age. For the models with two stellar populations, the burst strength is another free parameter that relates the mass of the young stars to the total mass of the galaxy. In addition to the stellar emission, we include the hydrogen gas emission in the form of nebular continuum and emission lines.

Once the galaxies with spectroscopic redshifts are fitted, they are used as templates for fitting the SEDs of those galaxies without a spectroscopic redshift. With the best model and best photometric redshift established, the stellar mass of the galaxy is obtained by scaling the models to the observed SED. The value of the stellar mass (M_*) is computed as the average of the stellar masses computed for each observed photometric band. Although most (52 out of 58) of the AGNs in our sample have spectroscopic redshifts (Szokoly et al. 2004; Vanzella et al. 2006), we refitted their SEDs using the library of templates. The stellar masses derived with the photometric redshift were then rescaled to the spectroscopic redshift.

As is discussed in great detail by Pérez-González et al. (2008), there are a variety of effects that can introduce systematic errors in the determination of stellar masses. In addition to the intrinsic uncertainties associated with fitting the SEDs (typically a factor of 2–3), other effects include the choices of stellar population libraries, extinction law, and IMF, as well as the number of stellar populations (in our case, one population vs. two populations). These effects introduce uncertainties that are on the order of or smaller than those intrinsic to the SED fitting.

Even though we selected our AGNs such that their SEDs are clearly dominated by stellar emission, the possible effect of the AGN emission in the determination of the stellar masses is a valid concern. In particular, such a concern was raised by Daddi et al. (2007) when estimating the stellar masses of $z \sim 2$ galaxies with MIR excesses that were thought to host obscured AGNs. These authors argued that the possible AGN contribution in the form of hot dust at $\lambda_{rest} \geq 1.6$ μm might cause overestimation of the stellar masses, but only at a modest level and generally within the systematic errors.

Daddi et al. (2007) estimated the stellar masses using empirical calibrations based on *B*-, *z*-, and *K*-band photometry. We believe our method is less susceptible to the effects of AGNs because we use population synthesis models to fit the entire observed SEDs, and the stellar masses are computed as the average of the stellar masses in all the photometric points. Pérez-González et al. (2008) discussed in detail the effects of the presence of a hot dust component (which could be associated with an AGN) in the determination of the stellar masses of AGNs. They concluded that the AGN effects on the estimated stellar masses are negligible for X-ray sources with observed (i.e., not corrected for absorption)

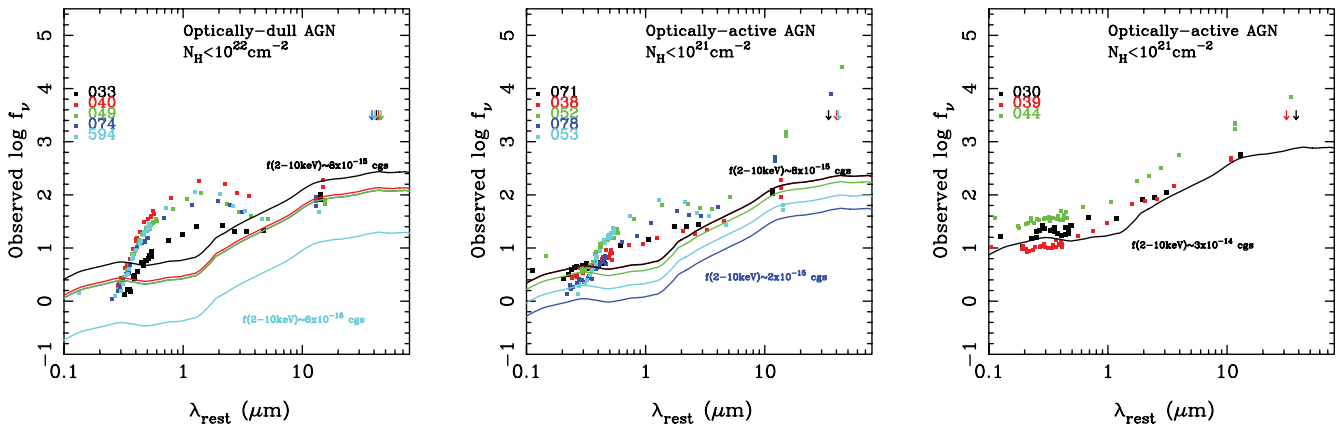

FIG. 3.—*Left*: Examples of rest-frame observed SEDs (in units of μJy; *filled squares*) of optically dull AGNs with low X-ray absorptions ($N_{\rm H} < 10^{22}$ cm^{-2}). For each galaxy, the Elvis et al. (1994) median quasar template (*solid line in the same color as the galaxy data points*) is plotted, scaled to the hard X-ray flux. These are those optically dull AGNs with low values of $N_{\rm H}$ for which the predicted AGN emission accounts for between approximately 30% and 100% of the observed 24 μm flux density. *Middle and right*: Examples of optically active AGNs in the same redshift interval studied here, also with low X-ray absorptions ($N_{\rm H} < 10^{21}$ cm^{-2}). In the middle panel, three AGNs (objects 52, 53, and 78 in Szokoly et al. 2004) are included in our sample of AGNs. Again, the Elvis et al. (1994) template is scaled to the observed hard X-ray flux of each AGN.

luminosities of $L_{\rm X} < 10^{44}$ erg s^{-1} (see also Donley et al. 2007). All the AGNs in our sample are well below this limit.

4. THE IR EMISSION

In this section, we evaluate whether the MIR emission of our sample of AGNs is likely to be due to the AGNs or to star formation. We then use the *Spitzer* data to model the total IR (8–1000 μm) luminosity ($L_{\rm IR}$) and to derive SFRs.

4.1. *The Observed* 24 μm *Emission of Low-*$N_{\rm H}$ *AGNs*

The X-ray column density can be used to classify AGNs into type 1 (direct view of the AGN; $N_{\rm H} < 10^{22}$ cm^{-2}) and type 2 (obscured view of the AGN). Rigby et al. (2004), using local AGN templates, showed that for low column densities, the 24 μm to hard X-ray flux ratio should remain approximately constant, whereas for high column densities this ratio varies by factors of a few. We test whether the 24 μm emission can be solely explained as being produced by dust heated by the putative AGN, or whether an additional mechanism (i.e., star formation) is needed. This is tested for the 18 optically dull AGNs (that is, those without evidence for accretion from the optical spectra) in our sample that have values of $N_{\rm H} < 10^{22}$ cm^{-2}. To do so, we scaled the median quasar template of Elvis et al. (1994) to the 2–10 keV flux (from Tozzi et al. 2006) for each of the 18 optically dull AGNs with low values of $N_{\rm H}$. The predicted AGN 24 μm flux densities were then compared with observed values.

We only find five optically dull AGNs with low values of $N_{\rm H}$ (Fig. 3, *left*) for which between 30% and 100% of their observed 24 μm flux densities could be accounted for with the predictions from their AGN hard X-ray fluxes. These five AGNs show the highest X-ray fluxes among the optically dull AGNs with low values of $N_{\rm H}$. For the rest (including some galaxies with $\lambda_{\rm rest} \sim$ 3–5 μm excesses), the predicted AGN 24 μm flux densities are below approximately 15% of the observed value, and thus most of their MIR emission is probably produced by star formation. In our analysis, we will assume that star formation dominates the 24 μm emission of these galaxies and of those that are similar except for having larger absorbing columns for their X-ray sources.

For comparison, the middle and right panels of Figure 3 show a few examples of the SEDs of optically active AGNs with $N_{\rm H} < 10^{21}$ cm^{-2} and their corresponding scaled quasar templates. The middle panel includes three optically active AGNs in our sample (objects 52, 53, and 78 in Szokoly et al. 2004). Only the MIR emission of one of them (object 53) is fully accounted for by the predictions from the AGN X-ray flux. From the right panel of Figure 3, it is clear that the AGN signatures (the UV bump and hot dust emission around $\lambda_{\rm rest} \sim 2$–5 μm and beyond) become dominant for the most X-ray–luminous AGNs (see, e.g., Barmby et al. 2006; Polletta et al. 2006, 2007; Donley et al. 2007).

4.2. *Modeling of the IR Emission*

After the stellar emission was modeled, as is described in § 3, the predicted stellar fluxes were subtracted from the observed photometric data points at $\lambda_{\rm rest} > 4$ μm. The resulting dust emission out to the MIPS 24 μm photometric point was then fitted using the Chary & Elbaz (2001) models to derive the IR luminosity. For the 24 μm nondetections (10 out of the 58 AGNs in our sample), the value of $L_{\rm IR}$ was computed by assuming an upper limit to the 24 μm flux density of 60 μJy, which is the 50% completeness limit of our catalog. The unobscured star formation is assumed to be traced by the UV monochromatic 2800 Å luminosity, as fitted by the stellar model. The total SFRs were computed as the sum of the IR and UV luminosities, which were converted to SFRs using the prescriptions of Kennicutt (1998).

Although we do not use the MIPS 70 μm photometric points to model the IR luminosities, we can check whether or not the f_ν(70 μm)/f_ν(24 μm) ratios or upper limits are consistent with star formation, as assumed. Only three optically dull AGNs are detected at 70 μm, all of which are in the $0.5 < z < 0.8$ bin (see Papovich et al. 2007 for more details). None of these three sources with 70 μm detections have observed f_ν(70 μm)/f_ν(24 μm) ratios that are consistent with those expected from hot dust arising from a νf_ν = constant distribution [f_ν(70 μm)/f_ν(24 μm) = 2.9, similar to optically selected quasars; Elvis et al. 1994; see Fig. 3; or AGN-dominated SEDs; see, e.g., Alonso-Herrero et al. 2006]. Neither are these colors consistent with those of IR-bright AGNs such as Mrk 231 [f_ν(70 μm)/f_ν(24 μm) $\sim$ 7–9, for our redshift range]. The behavior of the f_ν(70 μm)/f_ν(24 μm) ratio of optically dull AGNs is, however, similar to other sources (both detected and undetected in X-rays) in the same redshift range (see Papovich et al. 2007), as well as to empirical templates of local star-forming galaxies.

Since most of the optically dull AGNs with low absorptions have only modest X-ray luminosities ($L_{2-10\,\mathrm{keV}} < 2-3 \times 10^{42}$ erg s^{-1}; see Fig. 2), we consider the possibility that they do not contain an AGN, and thus that their X-ray luminosities could be produced by star formation. To do so, we can compare our total UV+IR SFRs with the SFRs predicted from their hard X-ray luminosities using the relation inferred by Ranalli et al. (2003). In all but one galaxy (object 577 in Szokoly et al. 2004, which is one of the galaxies with a high L_{IR}/M_* ratio), the X-ray–based SFRs would be between 3 and 10 times higher than our inferred value of $\mathrm{SFR}_{\mathrm{UV+IR}}$, indicating that in these galaxies most of the hard X-ray emission is not produced by star formation and that indeed they do contain a (low-luminosity) AGN.

4.3. *The Average Stellar Ages of the Host Galaxies*

In Figure 1, the observed SEDs (normalized at $\lambda_{\mathrm{rest}} = 1-2$ μm) are shown for the two redshift bins and are sorted according to their fitted L_{IR}/M_* ratios. If the AGN contribution to the MIR emission is small, these ratios are a good proxy for the specific SFRs (i.e., star formation rate per unit stellar mass). From the modeling of the stellar SEDs (see § 3), we find that most galaxies with high L_{IR}/M_* ratios are fitted with younger models than those with low L_{IR}/M_* ratios.

An independent way to estimate the average ages of the host galaxy stellar populations is to measure the 4000 Å break (see Kauffmann et al. 2003a, 2003b and references therein). The optical spectra (from Szokoly et al. 2004) of some $0.5 < z < 0.8$ AGNs with high and low L_{IR}/M_* ratios (as in Fig. 1) are shown in Figure 4.[7] The average $D_n(4000)$-values for the AGNs in Figure 4 with high and low L_{IR}/M_* ratios are $\sim$1.4 and $\sim$1.7, respectively. Thus, there is some marginal evidence for the AGN host galaxies with the lowest L_{IR}/M_* ratios to show larger 4000 Å breaks (i.e., older stellar populations) than the galaxies with high L_{IR}/M_* ratios. These $D_n(4000)$-values are similar to those of high-z AGNs identified by Kriek et al. (2007).

The measured $D_n(4000)$-values for our sample of AGNs indicate relatively young ages of between 0.8 and 2.5 Gyr for an instantaneous burst (using Fig. 2 of Kauffmann et al. 2003a). These ages, as well as the ages of local-universe type 2 AGNs (Kauffmann et al. 2003b) and intermediate-z type 1 AGNs (Sánchez et al. 2004), are younger than those of local quiescent massive galaxies, but consistent with the ages of IRAC-selected galaxies of similar masses (see Pérez-González et al. 2008).

Those galaxies in our sample (about one-third) with high L_{IR}/M_* ratios (Fig. 1, *left*) tend to show an excess of $\lambda_{\mathrm{rest}} \sim 3-5$ μm emission over the expectations of the stellar emission for an evolved stellar population. Although in most cases these MIR excesses can be accounted for by the gas + stellar emission associated with a young stellar population, we cannot rule out some contribution from warm dust emission associated with the putative AGNs. By our selection criteria (i.e., a prominent 1.6 μm stellar bump), the MIR excesses in our galaxies occur at $\lambda_{\mathrm{rest}} > 3$ μm, unlike the MIR-excess galaxies of Daddi et al. (2007) and IR power-law galaxies (Alonso-Herrero et al. 2006; Donley et al. 2007), in which the MIR excesses appear at $\lambda_{\mathrm{rest}} \sim 1.6$ μm. However, a large fraction (two-thirds) of the sample show no MIR excesses out to $\lambda_{\mathrm{rest}} \sim 5$ μm, with their MIR emission being entirely consistent with that of an evolved stellar population. Thus, in these galaxies the AGN emission appears to be completely buried out to $\lambda_{\mathrm{rest}} < 5$ μm, and possibly to longer wavelengths.

[7] At higher redshifts this feature is too close to the edge of their optical spectra.

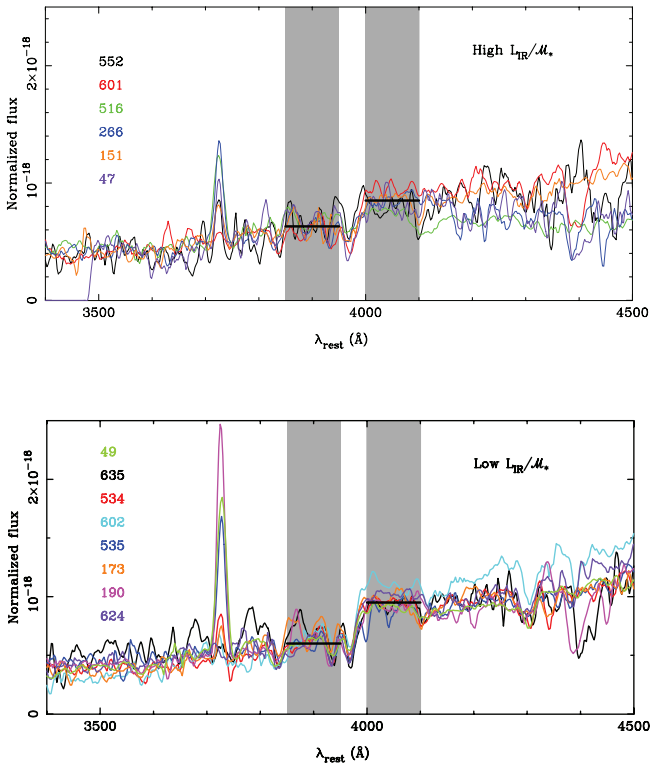

FIG. 4.—Normalized rest-frame spectra (from Szokoly et al. 2004) showing the spectral region of the [O II] λ3727 line and the 4000 Å break for AGNs in our sample at $0.5 < z < 0.8$. The shaded regions indicate the bandpasses that were defined by Balogh et al. (1999) to measure the $D_n(4000)$ index and that were used by Kauffmann et al. (2003a, 2003b) to derive the star formation histories of local AGNs. The thick lines in the bandpasses are plotted to guide the eye and correspond to the approximate average continuum level. The top and bottom panels show AGNs with high and low L_{IR}/M_* ratios (galaxies from the top left and top right panels of Fig. 1), respectively.

5. HOST GALAXY PROPERTIES

5.1. *Stellar Masses*

Figure 5 shows the stellar masses versus redshift for our sample of AGNs, compared with the distribution of stellar masses for the IRAC-selected sample of galaxies of Pérez-González et al. (2008). At the redshifts probed here, the IRAC-selected comparison sample is essentially a stellar mass–selected sample. Clearly, X-ray–selected AGNs reside in galaxies with a range of about an order of magnitude in mass, including some that are among the most massive at these intermediate redshifts. The characteristic stellar masses (measured as the median of the distributions) are 7.8×10^{10} $M_\odot$ (36 galaxies) at $0.5 < z < 0.8$ (median redshift of 0.67) and 1.2×10^{11} $M_\odot$ (22 galaxies) at $0.8 < z < 1.4$ (median redshift of 1.07). We also plot in Figure 5 as solid lines the redshift evolution of the quenching mass (the mass above which star formation should be mostly suppressed) inferred by Bundy et al. (2006), using two different methods. The fraction of AGNs above the line is small, perhaps indicating that star formation has not been fully suppressed yet in these galaxies (but see also § 5.2).

It is important to stress that the AGNs studied here comprise $\sim$50% of the X-ray–selected AGN population at $0.5 < z < 1.4$. A pressing question is whether the derived stellar masses are representative of the overall population of X-ray–selected AGNs. One possibility is that AGNs with stellar-dominated SEDs (mostly optically dull AGNs) might be hosted by massive galaxies (e.g., Moran et al. 2002; Severgnini et al. 2003; Caccianiga et al. 2007),

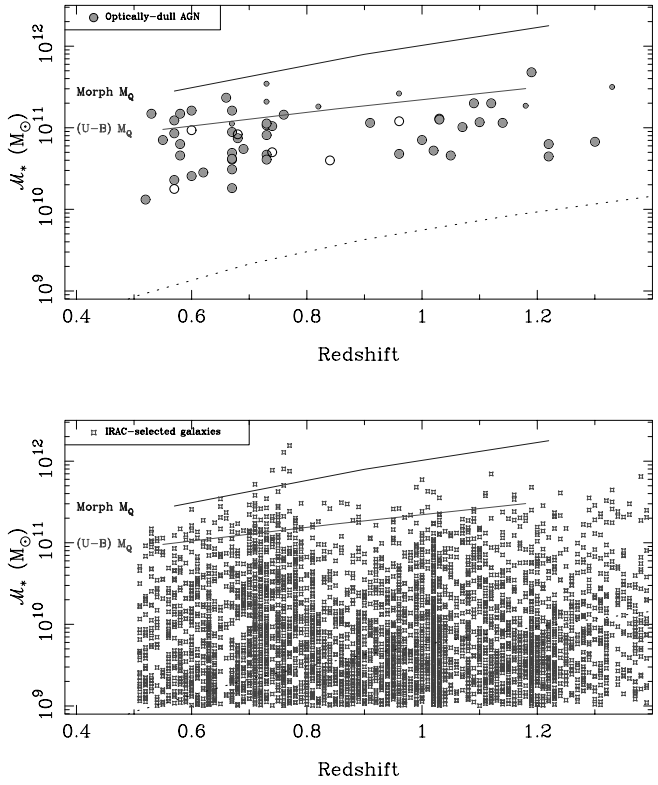

FIG. 5.— *Top*: Redshift evolution of the stellar mass of our sample of AGNs in the CDF-S (*circles*). We marked with small filled circles those optically dull AGNs with $M_* > 10^{11}\ M_\odot$ and that have specific SFRs that are similar to or below the median specific SFRs for IRAC-selected galaxies (see more details in § 5.2). The open circles indicate the stellar masses for the six optically active AGNs in our sample with stellar SEDs. The dotted line indicates the completeness limit of the sample of Pérez-González et al. (2008) for a maximally old passively evolving galaxy. The two solid lines show two empirical determinations (color and morphology) of the redshift evolution of the quenching mass (converted to a Salpeter IMF) from Bundy et al. (2006). *Bottom*: Redshift evolution of the stellar mass of IRAC-selected galaxies (Pérez-González et al. 2008) in the same field as our sample of CDF-S AGNs. The IRAC sample includes all the AGNs plotted in the top panel. Only galaxies with $M_* > 10^9\ M_\odot$ are plotted in this comparison. [*See the electronic edition of the Journal for a color version of this figure*.]

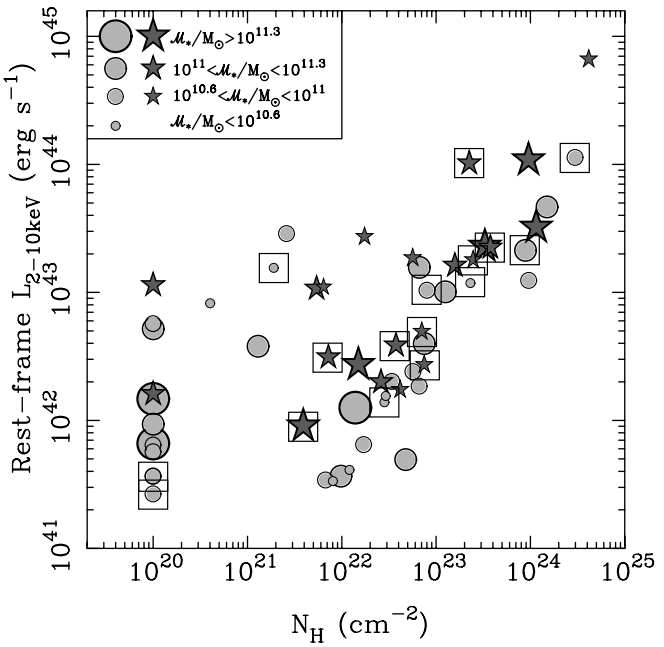

FIG. 6.— Similar to Fig. 2, but for only the AGNs selected for this study, which are coded according to their derived stellar masses for the two redshift bins considered here ($0.5 < z < 0.8$, *circles*; $0.8 < z < 1.4$, *stars*). We also marked with squares those optically dull AGNs with $\lambda_{rest} \sim 3$–$5\ \mu$m excesses over pure stellar emission from an old stellar population (Fig. 1, *left*). [*See the electronic edition of the Journal for a color version of this figure*.]

causing the AGN emission lines to be buried by the galaxy emission. To test this possibility, in Figure 6, which is similar to Figure 2, the AGNs in our sample are sorted according to their stellar masses. There is no clear tendency for the most X-ray–luminous sources to be hosted by the most massive galaxies. As demonstrated by Rigby et al. (2006), extinction on large scales produced by the host galaxy might also be responsible for hiding the AGN lines in these galaxies.

Ideally, we would like to estimate the stellar masses for all optically active AGNs at intermediate redshifts, but this becomes increasingly more uncertain (see Pérez-González et al. 2008), as for more luminous X-ray sources the AGN emission in the optical–NIR becomes more dominant (e.g., Barmby et al. 2006; Polletta et al. 2006, 2007; Donley et al. 2007; see also § 4.1). The masses of the six optically active AGNs in our sample do not appear to be fundamentally different from those of optically dull AGNs (see Fig. 5), although the number statistics are very small.

Another way to determine if the stellar masses of optically dull AGNs are representative is to compare their absolute magnitudes with those of optically active AGNs. If both types of AGNs reside in similar systems, then optically active AGNs should be more luminous in the optical and near-IR because they should have the contributions from the host galaxy and the AGN. Rigby et al. (2006; see their Fig. 8) already made this comparison, and they found that broad-line AGNs (BLAGNs) with $L_X > 10^{43}$ erg s^{-1} tend to show brighter optical magnitudes than do optically dull AGNs of similar luminosities. Again, the number statistics are small, but both comparisons seem to suggest that the stellar masses of optically dull AGNs are representative of the whole X-ray–selected AGN population at these redshifts.

Optically selected type 2 AGNs at $z < 0.3$ are also found to reside in the most massive galaxies. Kauffmann et al. (2003b) inferred a characteristic stellar mass of ~ 4–$5 \times 10^{10}\ M_\odot$ (for a Salpeter IMF) for bright type 2 AGNs (see also Heckman et al. 2004). At high redshifts ($z \sim 2$), X-ray–selected AGNs appear to be hosted by even more massive galaxies ($M_* \sim 1$–$2 \times 10^{11}\ M_\odot$), although the mass estimates have only been done for a few galaxies (see Borys et al. 2005; Daddi et al. 2007; but see also caveats discussed by Alexander et al. 2007). Similarly, Kriek et al. (2007) find that $z \sim 2.3$ AGNs identified in K band–selected galaxies are hosted by very massive galaxies, but, as they point out, it is likely that their results are biased toward the most massive objects. The stellar masses of AGNs at $z \sim 0.7$ and $z \sim 1.1$ are thus intermediate between those of local AGNs and high-z AGNs.

Since the stellar masses of our sample of AGNs appear to be representative of the whole population of X-ray–selected AGNs (see Fig. 5), we infer that approximately 25% of massive galaxies ($M_* > 10^{11}\ M_\odot$) at the redshifts probed here contain an X-ray–identified AGN. We also took into account AGNs not included in this study, assuming that they have stellar masses similar to the AGNs with stellar-dominated SEDs. This fraction is similar for the two redshift bins considered here and is consistent with the AGN fraction in massive galaxies at higher redshifts ($z > 1$; Alexander et al. 2005; Daddi et al. 2005; Papovich et al. 2006; Kriek et al. 2007). Our estimated AGN fraction in intermediate-z massive galaxies is only a lower limit, because presumably most Compton-thick AGNs are missed by current X-ray surveys. At $z \sim 2$ the fraction of AGNs in massive galaxies appears to be as high as 50%–60% (Daddi et al. 2007), consistent with the view

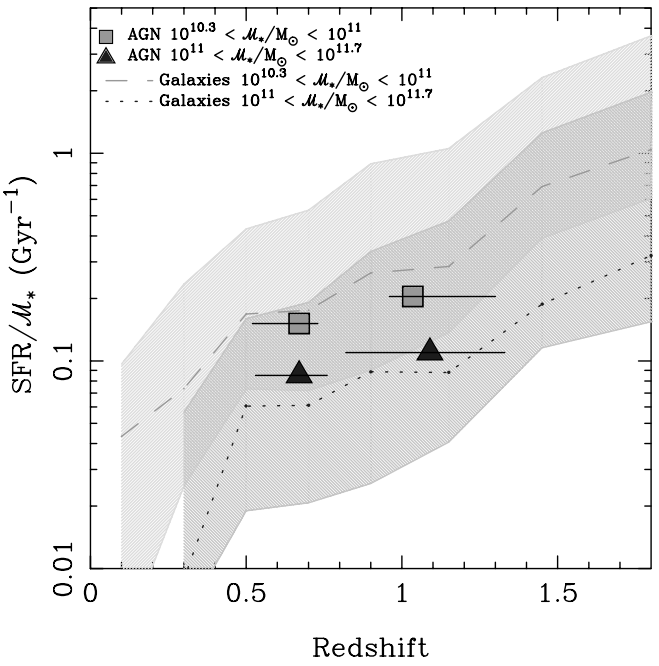

FIG. 7.—Redshift evolution of the specific SFR for IRAC-selected galaxies in a number of cosmological fields. This figure is an updated version (it now includes additional data for the extended Groth strip; P. Pérez-González et al. 2008, in preparation) of Fig. 10 by Pérez-González et al. (2008), but here we only show the mass intervals that are of interest for our sample of AGNs. The dashed and dotted lines represent the median specific SFRs for the $2 \times 10^{10}\ M_\odot < M_* < 10^{11}\ M_\odot$ and $10^{11}\ M_\odot < M_* < 5 \times 10^{11}\ M_\odot$ mass ranges, respectively. We also show the quartiles of the distribution of specific SFRs of IRAC-selected galaxies for each of the two mass ranges as the shaded regions. The median specific SFRs for AGNs are shown by the filled squares and triangles plotted at the median redshift. The horizontal bars represent the ranges of redshifts. We excluded AGNs that had MIR excesses or that were classified as optically active. [*See the electronic edition of the Journal for a color version of this figure.*]

that massive black hole growth was higher when the universe was younger.

5.2. *Star Formation Activity*

In this section we quantify the star formation activity of AGNs with stellar-dominated SEDs in relation to that of IRAC-selected galaxies of similar stellar masses and at similar redshifts. We use the specific SFRs as an indicator of the star formation activity rather than the absolute SFRs, as the specific SFR measures the rate at which new stars add to the assembled mass of the galaxy (Brinchmann & Ellis 2000). Moreover, galaxies show distinct specific SFRs, depending on their stellar masses and redshifts (e.g., Brinchmann et al. 2004; Zheng et al. 2007; Pérez-González et al. 2008), so the comparison needs to be made with this taken into account.

Figure 7 compares the median specific SFRs for intermediate-z AGNs with those of the IRAC-selected sample of Pérez-González et al. (2008). In this comparison we excluded MIR-excess galaxies and the six optically active AGNs, as they may have an important AGN contribution to their observed MIR emission that would cause us to overestimate their IR-based SFRs. The comparison between AGNs and IRAC-selected galaxies is done for the two relevant stellar mass ranges of the AGN hosts (see Fig. 5): $2 \times 10^{10}\ M_\odot < M_* < 10^{11}\ M_\odot$ and $10^{11}\ M_\odot < M_* < 5 \times 10^{11}\ M_\odot$.

As can be seen from Figure 7, the AGN specific SFRs (at both redshift and mass intervals) do not appear to be fundamentally different from those of IRAC-selected galaxies. Moreover, Zheng et al. (2007) argued against AGN feedback as the main process for quenching star formation. Their model predicted that AGN feedback would be more effective for more massive galaxies (see also Croton et al. 2006). This would imply a more rapid decline of the specific SFR for massive galaxies ($>10^{11}\ M_\odot$) than for less massive galaxies (see also Springel et al. 2005), which is observed neither for the Zheng et al. (2007) sample nor for the IRAC-selected sample of Pérez-González et al. (2008; see Fig. 7).

In contrast, Kriek et al. (2007) found evidence for a relation between the suppression of star formation and the AGN phase for K band–selected galaxies. Kriek et al. (2007), however, pointed out that their AGN sample may be biased toward quiescent galaxies where AGNs are easier to identify. In fact, if we consider their two samples of galaxies (UV- and K band–selected), then the AGNs have specific SFRs that are within the range observed for their non-AGNs. In the local universe, AGNs tend to be hosted in massive galaxies with younger stellar ages than do non-AGNs of similar morphological types (early type) and stellar masses (Kauffmann et al. 2003a, 2007). This was interpreted as evidence that enhanced star formation is a requisite for feeding the AGNs. At $z \sim 1$, galaxies (presumably both AGNs and non-AGNs) with $M_* \sim 10^{10}$–$5 \times 10^{11}\ M_\odot$ are still being assembled (see Pérez-González et al. 2008), so perhaps it is not surprising that their star formation rates are not significantly different.

5.2.1. *Caveats*

There are a number of caveats that we must consider when trying to assess the star formation activity of our sample of AGNs. As has been discussed in previous sections, there is the exact AGN contribution to the MIR emission, although it is found generally not to be large (§ 4.1). Also, the AGNs in the $0.8 < z < 1.4$ redshift range tend to be more luminous in X-rays, so the AGNs become more apparent. Even though we excluded galaxies with MIR excesses (as we cannot rule out that these excesses might be due to dust heated by the AGNs), the specific SFRs are formally upper limits. Another largely unknown effect in the comparison between AGNs and IRAC-selected galaxies is the possible "contamination" by X-ray–identified AGNs, as well as obscured AGNs, in the most massive ($M_* > 10^{11}\ M_\odot$) systems (see § 5.1; Daddi et al. 2007; Kriek et al. 2007) in the comparison sample.

Another concern is the possibility that the obscuring material, which may be responsible in part for the optical dullness, might be associated with star formation activity within the host galaxy (e.g., Ballantyne et al. 2006; Martínez-Sansigre et al. 2006). This would bias our sample toward star-forming galaxies when compared to the most optically active AGNs not included in our sample. Figure 8 shows a comparison between the derived UV+IR SFRs and the X-ray absorption for our sample of AGNs. This figure suggests a weak connection, if any, between star formation and obscuration. It is also clear that a number of highly obscured AGNs ($N_{\rm H} > 10^{22}\ {\rm cm}^{-2}$) do not present high SFRs, and in these cases the obscuration is probably not associated with extranuclear dust in the host galaxy.

To summarize, at intermediate z we do not find strong evidence for either highly suppressed star formation activity or increased star formation activity in AGNs when compared to IRAC-selected galaxies of similar stellar masses. We only observe that the most massive galaxies with low specific SFRs (see Fig. 5) follow the redshift evolution of the quenching mass inferred by Bundy et al. (2006). This may only indicate that the most massive systems hosting an AGN are close to being fully assembled at these redshifts.

6. BLACK HOLE MASSES AND ACCRETION RATES OF TYPICAL AGNs

The relation between the black hole mass and the bulge luminosity and in particular the bulge stellar mass is now well established

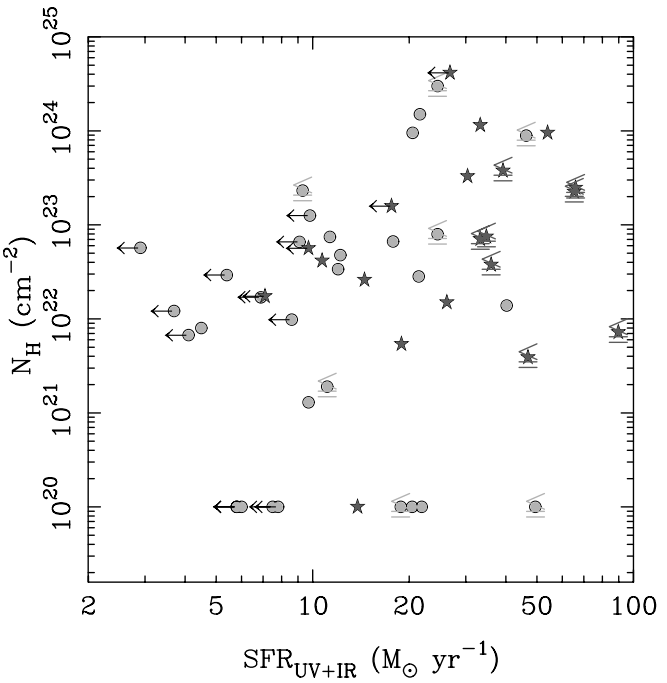

FIG. 8.— Total SFR vs. X-ray column densities for the sample of optically dull AGNs. Symbols are as in Fig. 6 for the two redshift bins. The SFRs of galaxies with 24 μm flux densities below 80 μJy are marked as upper limits. Galaxies with rest-frame 3–5 μm excesses (left panels of Fig. 1) are shown with the "less than or equal" symbols, as their MIR emission might include some AGN contributions. [*See the electronic edition of the Journal for a color version of this figure.*]

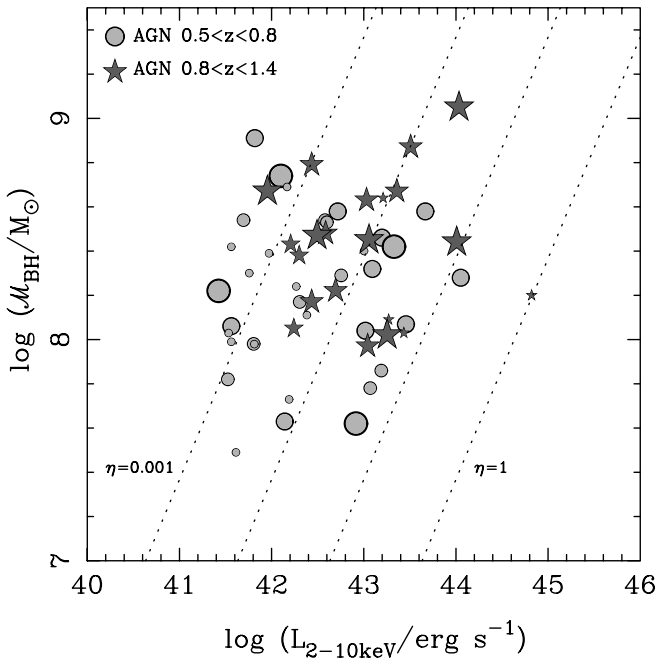

FIG. 9.— Black hole masses (derived from the M_{BH}/M_{bulge} relation of Marconi & Hunt 2003) vs. absorption-corrected rest-frame hard X-ray luminosities. The circles indicate AGNs at $0.5 < z < 0.8$, and the star symbols indicate AGNs at $0.8 < z < 1.4$. The sizes of the symbols are proportional to their rest-frame 24 μm luminosities. For both redshift bins, the smallest symbols represent galaxies that were not detected at 24 μm or that have flux densities below 80 μJy. The dotted lines indicate, from right to left, Eddington ratios of $\eta = 1$, 0.1, 0.01, and 0.001, with the assumption of a bolometric correction of $L_{bol}/L_X \sim 30$ as derived by Elvis et al. (1994). [*See the electronic edition of the Journal for a color version of this figure.*]

in the local universe (e.g., Merritt & Ferrarese 2001; Marconi & Hunt 2003). This relationship appears to hold out to $z \sim 1$ (Peng et al. 2006), indicating that massive bulges were fully assembled at this redshift (see, e.g., Glazebrook et al. 2004; Cimatti et al. 2004; Papovich et al. 2006; Pérez-González et al. 2008). Since the AGN activity out to $z \sim 1.3$ seems to be associated with bulge-dominated galaxies (see Sánchez et al. 2004; Grogin et al. 2005; Pierce et al. 2007), we can use the local relationship and our stellar masses to estimate the black hole masses of intermediate-z AGNs.

Using the Marconi & Hunt (2003) relation and assuming that $M_{bulge} \approx M_*$, we find black hole masses for typical AGNs of approximately between 4×10^7 and 10^9 $M_\odot$, with a median value of $M_{BH} \sim 2 \times 10^8$ $M_\odot$. These are in good agreement with the estimates of Babić et al. (2007) for CDF-S $z \sim 0.7$ AGNs, which were based on stellar masses and stellar velocity dispersions. The resulting values of M_{BH} for optically dull AGNs are plotted in Figure 9 against the absorption-corrected rest-frame hard X-ray luminosities.[8]

In Figure 9 we also show the Eddington ratios ($\eta = L_{bol}/L_{Edd}$) calculated using the bolometric corrections ($L_{bol}/L_X \sim 30$) derived for Palomar-Green (PG) quasars by Elvis et al. (1994). Optically dull AGNs at $0.5 < z < 1.4$ with X-ray luminosities above 10^{43} erg s^{-1} have Eddington ratios close to those of broad-line AGNs ($\sim$0.16; Barger et al. 2005). However, for X-ray luminosities below 10^{43} erg s^{-1} (comparable to local Seyfert galaxies), the Eddington ratios are much lower ($\eta \sim 0.01$–0.001, similar to the findings of Babić et al. 2007).

[8] The sizes of the symbols are proportional to their rest-frame monochromatic 24 μm luminosities. If most of the MIR emission was produced by dust heated by an AGN, one would expect a proportionality between the absorption-corrected X-ray luminosities (a proxy for the AGN luminosity) and the MIR luminosities, which is not observed in general for optically dull AGNs (see also Rigby et al. 2006). This again suggests that a large fraction of the MIR emission relative to the AGN luminosity could be due to star formation.

One possibility for the low Eddington ratios is that we were significantly overestimating the black hole masses: for instance, if these galaxies were not bulge-dominated. However, the corrections to the bulge masses (and thus the black hole masses) would be on the order of $\sim$2 and $\sim$5–6 if the morphological types were S0/a and Sc, respectively (see, e.g., Marconi et al. 2004; Dong & De Robertis 2006), if we assume that the NIR luminosity traces the stellar mass. Recently, Ballo et al. (2007) derived bulge magnitudes for X-ray sources in the CDF-S and found that in general, in the ACS z band, the ratios of bulge luminosity to total luminosity are between 0.4 and 1. For the two sources in our sample that are in common with theirs, these ratios are 0.6–0.8. From this, the black hole masses quoted here should be taken as upper limits and the Eddington ratios as lower limits, although the corrections are likely to be relatively small.

The AGN hosts in our sample follow very well the redshift evolution of the quasar host mass derived by Hopkins et al. (2007) from the quasar optical luminosity function. This is interesting, because our AGNs are not X-ray quasars (i.e., $L_X < 10^{44}$ erg s^{-1}; see Fig. 2). This is also indirect evidence that the accretion rates of optically dull AGNs are lower than those of bright quasars. In § 5.1, on the other hand, we found that the characteristic stellar masses of intermediate-z AGNs are between those of local AGNs and high-z ($z > 2$) AGNs. This would appear to support the interpretation of Heckman et al. (2004) for the AGN "downsizing" phenomenon. In this scenario, the fact that the space density of low-luminosity AGNs peaks at lower redshifts than that of more luminous AGNs (see Ueda et al. 2003) is explained by a decrease of the characteristic mass of actively accreting black holes (and thus the stellar mass of the host) rather than by a decreasing accretion rate (see also Barger et al. 2005). Since it is these low X-ray

luminosity AGNs that dominate the X-ray background at the redshifts considered here, the AGN "downsizing" is not only due to a decrease in the characteristic stellar mass (see § 5.1), but also to lower Eddington ratios.

7. SUMMARY AND CONCLUSIONS

We studied a sample of 58 X-ray–selected AGNs at intermediate redshifts ($z \sim 0.5$–1.4) in the GOODS portion of the CDF-S. The AGNs were selected such that their rest-frame UV to NIR SEDs were dominated by stellar emission and, in particular, showed a prominent 1.6 μm bump. This selection minimized the AGN contamination, which is essential when studying the properties of their host galaxies. Since AGNs with stellar-dominated SEDs comprise approximately 50% of the population of X-ray–selected AGNs, they are a cosmologically important class of AGNs. We fitted their rest-frame UV through MIR SEDs, using stellar and dust models to derive the stellar masses, as well as the total (UV+IR) SFRs.

As previously discussed in other works (e.g., Severgnini et al. 2003; Rigby et al. 2006; Caccianiga et al. 2007), the optical dullness might be due to various causes. We find that dilution by a massive host galaxy is only in part responsible, as the mass of the host galaxy is independent of the X-ray luminosity and absorption of the AGN. Extinction on large scales may also play a role, and this is presumably relatively prevalent in the lower mass optically dull AGN hosts. From this and the derived stellar masses of a few optically active AGNs with stellar SEDs, we conclude that the derived stellar masses of our sample of AGNs are representative of the entire X-ray–selected AGN population at these redshifts.

About one-third of our AGNs show $\lambda_{\rm rest} \sim 3$–$5$ μm excesses above the expected stellar emission from an old stellar population, together with high $L_{\rm IR}/M_*$ ratios. Although these MIR excesses could be interpreted as evidence for the putative AGNs (i.e., hot dust), these galaxies tend to have smaller 4000 Å breaks. That is, galaxies with MIR excesses have younger average stellar populations (an indication of recent or ongoing star formation) than do galaxies with low $L_{\rm IR}/M_*$ ratios. This may indicate that AGN emission is responsible for most of the MIR emission only in some galaxies. For the rest of the sample, there is no evidence for AGN emission out to approximately $\lambda_{\rm rest} \sim 5$ μm, and the MIR emission of these galaxies is likely to be produced mostly by star formation.

X-ray–identified AGNs are found to reside in galaxies with a range of stellar masses ($M_* \sim 2 \times 10^{10}$–$5 \times 10^{11}$ $M_\odot$, for a Salpeter IMF), including the most massive galaxies at intermediate redshifts. We infer characteristic (median) stellar masses of $M_* \sim 7.8 \times 10^{10}$ and $M_* \sim 1.2 \times 10^{11}$ $M_\odot$ at median redshifts of 0.67 and 1.07, respectively. These stellar masses are intermediate between those of local type 2 AGNs ($\sim 4 \times 10^{10}$ $M_\odot$; Kauffmann et al. 2003b) and high-z AGNs (~ 1–3×10^{11} $M_\odot$; Kriek et al. 2007; Daddi et al. 2007; Alexander et al. 2007). From a comparison with the IRAC-selected sample of Pérez-González et al. (2008), we find that approximately 25% of massive ($M_* > 10^{11}$ $M_\odot$) galaxies at these redshifts contain an X-ray–identified AGN.

Using the local relation between $M_{\rm bulge}$ and $M_{\rm BH}$ of Marconi & Hunt (2003), we find that the inferred black hole masses ($M_{\rm BH} \sim 2 \times 10^8$ $M_\odot$) are similar to those of broad-line AGNs, although with lower Eddington ratios ($\eta \sim 0.01$–0.001) than luminous quasars. Both findings suggest that, at least at intermediate redshifts, the cosmic AGN "downsizing" is probably due not only to a decrease in the characteristic stellar mass of the host galaxy (as proposed by Heckman et al. 2004), but also to less efficient accretion, as was also found by Babić et al. (2007).

Finally, we do not find strong evidence in AGN host galaxies for either highly suppressed star formation (which would be expected if AGNs played a role in quenching star formation) or intense star formation when compared to IRAC-selected galaxies of similar stellar masses and redshifts. This can be understood if we take into account the fact that the host galaxies of AGNs (and non-AGNs of similar mass) are still being assembled at the redshifts probed here. The main caveats regarding this conclusion are the possible influence on it of the AGN contribution to the observed MIR emission (although this is found generally not to be large) and the possible bias toward intense star formation, which could be in part responsible for obscuring the AGNs in these objects.

The authors would like to thank P. Hopkins and M. Kriek for interesting discussions. The authors also thank an anonymous referee for useful suggestions that helped improve the paper. This work was supported by NASA through contract 1255094 issued by the JPL/California Institute of Technology. A. A.-H. acknowledges support from the Spanish Plan Nacional del Espacio under grant ESP2005-01480. P. G. P.-G. acknowledges support from the Ramón y Cajal Fellowship Program financed by the Spanish Government, and from the Spanish Programa Nacional de Astronomía y Astrofísica under grant AYA 2006-02358. This research has made use of the NASA/IPAC Extragalactic Database (NED), which is operated by the Jet Propulsion Laboratory, California Institute of Technology, under contract with the National Aeronautics and Space Administration.

REFERENCES

Alexander, D. M., Smail, I., Bauer, F. E., Chapman, S. C., Blain, A. W., Brandt, W. N., & Ivison, R. J. 2005, Nature, 434, 738
Alexander, D. M., et al. 2003, AJ, 126, 539
———. 2007, ApJ, submitted
Alonso-Herrero, A., et al. 2006, ApJ, 640, 167
Babić, A., Miller, L., Jarvis, M. J., Turner, T. J., Alexander, D. M., & Croom, S. M. 2007, A&A, 474, 755
Ballantyne, D., Everett, J. E., & Murray, N. 2006, ApJ, 639, 740
Ballo, L., et al. 2007, ApJ, 667, 97
Balogh, M. L., Morris, S. L., Yee, H. K. C., Carlberg, R. G., & Ellingson, E. 1999, ApJ, 527, 54
Barger, A. J., Cowie, L. L., Mushotzky, R. F., Yang, Y., Wang, W.-H., Steffen, A. T., & Capak, P. 2005, AJ, 129, 578
Barger, A. J., et al. 2003, AJ, 126, 632
Barmby, P., et al. 2006, ApJ, 642, 126
Bell, E. F., Zheng, X. Z., Papovich, C., Borch, A., Wolf, C., & Meisenheimer, K. 2007, ApJ, 663, 834
Bell, E. F., et al. 2004, ApJ, 608, 752
Borys, C., Smail, I., Chapman, S. C., Blain, A. W., Alexander, D. M., & Ivison, R. J. 2005, ApJ, 635, 853
Brandt, W. N., & Hasinger, G. 2005, ARA&A, 43, 827
Brinchmann, J., Charlot, S., White, S. D. M., Tremonti, C., Kauffmann, G., Heckman, T., & Brinkmann, J. 2004, MNRAS, 351, 1151
Brinchmann, J., & Ellis, R. S. 2000, ApJ, 536, L77
Bundy, K., et al. 2006, ApJ, 651, 120
Caccianiga, A., Severgnini, P., Della Ceca, R., Maccacaro, T., Carrera, F. J., & Page, M. J. 2007, A&A, 470, 557
Calzetti, D., Armus, L., Bohlin, R. C., Kinney, A. L., Koornneef, J., & Storchi-Bergmann, T. 2000, ApJ, 533, 682
Chary, R., & Elbaz, D. 2001, ApJ, 556, 562
Cimatti, A., et al. 2004, Nature, 430, 184
Cohen, J. G. 2003, ApJ, 598, 288
Croton, D. J., et al. 2006, MNRAS, 365, 11
Daddi, E., et al. 2005, ApJ, 626, 680
———. 2007, ApJ, 670, 173
Dong, X. Y., & De Robertis, M. M. 2006, AJ, 131, 1236

Donley, J. L., Rieke, G. H., Pérez-González, P. G., Rigby, J. R., & Alonso-Herrero, A. 2007, ApJ, 660, 167
Elvis, M., et al. 1994, ApJS, 95, 1
Fazio, G. G., et al. 2004, ApJS, 154, 10
Fioc, M., & Rocca-Volmerange, B. 1997, A&A, 326, 950
Giacconi, R., et al. 2002, ApJS, 139, 369
Glazebrook, K., et al. 2004, Nature, 430, 181
Grogin, N. A., et al. 2005, ApJ, 627, L97
Heckman, T. M., Kauffmann, G., Brinchmann, J., Charlot, S., Tremonti, C., & White, S. D. M. 2004, ApJ, 613, 109
Hopkins, P. F., Bundy, K., Hernquist, L., & Ellis, R. S. 2007, ApJ, 659, 976
Kauffmann, G., et al. 2003a, MNRAS, 341, 33
———. 2003b, MNRAS, 346, 1055
———. 2007, ApJS, 173, 357
Kennicutt, R. C., Jr. 1998, ARA&A, 36, 189
Kriek, M., et al. 2007, ApJ, 669, 776
Lacy, M., et al. 2004, ApJS, 154, 166
Marconi, A., & Hunt, L. K. 2003, ApJ, 589, L21
Marconi, A., Risaliti, G., Gilli, R., Hunt, L. K., Maiolino, R., & Salvati, M. 2004, MNRAS, 351, 169
Martin, D. C., et al. 2007, ApJS, 173, 342
Martínez-Sansigre, A., Rawlings, S., Lacy, M., Fadda, D., Jarvis, M. J., Marleau, F. R., Simpson, C., & Willott, C. J. 2006, MNRAS, 370, 1479
Merritt, D., & Ferrarese, L. 2001, MNRAS, 320, L30
Moran, E. C., Filippenko, A. V., & Chornock, R. 2002, ApJ, 579, L71
Nandra, K., et al. 2007, ApJ, 660, L11
Papovich, C., et al. 2006, ApJ, 640, 92
Papovich, C., et al. 2007, ApJ, 668, 45
Peng, C. Y., Impey, C. D., Rix, H.-W., Kochanek, C. S., Keeton, C. R., Falco, E. E., Lehár, J., & McLeod, B. A. 2006, ApJ, 649, 616
Pérez-González, P. G., et al. 2005, ApJ, 630, 82
———. 2008, ApJ, 675, 234
Pierce, C. M., et al. 2007, ApJ, 660, L19
Polletta, M. C., et al. 2006, ApJ, 642, 673
———. 2007, ApJ, 663, 81
Ranalli, P., Comastri, A., & Setti, G. 2003, A&A, 399, 39
Rieke, G. H., et al. 2004, ApJS, 154, 25
Rigby, J. R., Rieke, G. H., Donley, J. L., Alonso-Herrero, A., & Pérez-González, P. G. 2006, ApJ, 645, 115
Rigby, J. R., et al. 2004, ApJS, 154, 160
Salim, S., et al. 2007, ApJS, 173, 267
Salpeter, E. E. 1955, ApJ, 121, 161
Sánchez, S. F., et al. 2004, ApJ, 614, 586
Severgnini, P., et al. 2003, A&A, 406, 483
Springel, V., Di Matteo, T., & Hernquist, L. 2005, MNRAS, 361, 776
Stern, D., et al. 2005, ApJ, 631, 163
Szokoly, G. P., et al. 2004, ApJS, 155, 271
Tozzi, P., et al. 2006, A&A, 451, 457
Ueda, Y., Akiyama, M., Ohta, K., & Miyaji, T. 2003, ApJ, 598, 886
Vanzella, E., et al. 2005, A&A, 434, 53
Zheng, W., et al. 2004, ApJS, 155, 73
Zheng, X. Z., Bell, E. F., Papovich, C., Wolf, C., Meisenheimer, K., Rix, H.-W., Rieke, G. H., & Somerville, R. 2007, ApJ, 661, L41